Investigating the Effect of Optimum Welding Parameters on the Microstructural and Mechanical Properties of St37 Steel and 316L Stainless Steel Welded by the Friction Stir Welding Process

R. Amini Najafabadi [*1], F. Salehi [2], T. Isfahani [3]

[1, 3] Department of Materials Science and Engineering, Golpayegan University of Technology, Golpayegan, Iran
[2] Metallurgy & Materials Engineering Dept., Golpayegan University of Technology, Golpayegan, P. O. Box: 87717-65651 Iran

Abstract

In this research, St37 and 316L steel sheets were welded using friction stir welding (FSW) process and effective parameters such as the rotational speed, linear speed of the tool, pin diameter and their appropriate values were studied. The microstructure, hardness, and strength of the different welding regions were investigated. It was observed that in the stir zone (SZ), a mechanical operation takes place which causes grain refinement up to 10-20 times and improves the mechanical properties of the joint. The thermo-mechanically affected zone (TMAZ) is less affected and causes the refinement of the structure. In the heat affected zone (HAZ), no mechanical operation was performed but in some parts, the grain size was larger and more stretched than the grains of the base metal. SEM microscopic images of the weld metal showed alternating onion rings and layers consisting of poor and rich alloying elements due to the non-equilibrium cooling rate of the melt.

Keywords: Friction stir welding (FSW); Steel; 316L; St37; Microstructure.

1. Introduction

Friction-Stir Welding (FSW) introduced by TWI welding institute in 1991 is a comparatively new welding process [1)] and was developed in Sweden by ESAB company [2)]. This process turned on the spotlight towards non-traditional, solid state and thermo-mechanical joining process [3)]. This new method of production has been used in order to achieve the required products more quickly [4)] . FSW has been widely investigated and was initially commercialized mostly for low temperature melting materials such as Al, Mg and Cu alloys. Later, this process was used for joining steel and aluminum sheets especially in automotive industries [5-7)]. The principle of this process is that the jointing takes place at high strain rates due to combined processes such as heating by friction, mixing of plasticized material from either side, forging by shoulder and extrusion along the weld line with a tilt angle [3)]. This results in mechanical properties superior to other welding processes. The welding's obtained by FSW are usually free of defects. However, the main problem of this process is that some mechanical properties such as the strength relative to the base metal may decrease [8)].

Research has shown that it is possible to obtain con-

**Corresponding author*
Email: reza.amini@mail.ru
Address: Metallurgy & Materials Engineering Dept., Golpayegan University of Technology, Golpayegan, P. O. Box: 87717-65651 Iran
1. Assistant Professor
2. M.Sc.
3. Assistant Professor

venient mechanical properties by selecting appropriate parameters such as the velocity of the tool rotation, tool progressing speed, pin diameter and tool shoulder and also (though with a lower degree of importance) by properly choosing the angle of deviation, pre-heating, tool rotation direction (clockwise or anti-clockwise), fastening system, tool geometry, etc.[9]. In high temperature applications such as vapor lines of power plants, heat exchangers, nuclear reactors and petrochemical industries sections exist which are also subject to low temperatures. Therefore, the sections in contact with high temperatures are usually made from austenite stainless steel while the sections of low temperature are from low carbon steel. The reason of using low carbon steel is that it has good mechanical properties along with a low cost [10]. Up to now, several conventional methods have been used to produce dissimilar welding such as GTAW, RSW, FW, LSW and EBW which usually result in low mechanical properties while FSW has not been extensively studied for most cases. Therefore, there seems to be a demand for obtaining other ways to increase the mechanical properties of the welded parts.

S. Meran et al. examined FSW of 304L austenitic stainless steel. They determined the optimum parameters, mechanical properties, and the microstructure [11]. In another study, Y. Sankara et al. conducted a study to improve the 6061 aluminum friction stir welding parameters using the Design Expert software [12]. They determined the optimum parameters by examining the mechanical properties [13].

Up to our knowledge, no research has been presented on the frictional welding of St37 and 316 L stainless steel sheets by FSW. Due to the advantages of the FSW process, increasing the mechanical properties of these welds is possible. Considering the importance of the subject, in this study, while specifying the optimum parameters of the friction stir welding of St37 stainless steel sheets and 316 L stainless steel, the microstructure resulting from the joining by the FSW process and its mechanical properties are investigated. For this reason, optimum welding parameters have been obtained by using the design of experiments (DOE) method. The DOE has been used in several studies to improve the quality of data and obtain the optimum conditions [14-18]

2. Materials and Method

St37 and 316L sheets with a thickness of 1.5mm were selected to be connected by butt jointing without any chamfer and gap. First, the sheets were cut into 160 × 80 mm dimensions, and then the burrs were removed by a rasp. A special fixture was designed and built for welding the sheets by FSW. At the beginning, to find out the upper and lower levels of the linear and rotational speed, several experiments were applied according to other published research [6, 18] and a shoulder tool with 14 mm diameter with a conical pin was supplied. Material of the used tool was tungsten carbide, produced by powder metallurgy (BK2, Russia). In the welding of all samples, the used tools were constant. Using the manufactured tool, the effect of rotational and linear traveling speed on the strength of the produced plates was investigated. The rotational speed of the tool, speed of the linear travel and diameter of the pin tool were assumed as the controllable variable parameters and other parameters like the deviation angle, shoulder tool diameter, pin length, etc. were assumed as the fixed controllable parameters. Applying the friction stir welding process to joint sheets of any alloying group with any thickness requires laboratory examinations to be applied in order to determine the upper and lower levels of the rotational speed and linear speed travel of tools. Laboratory experiments were used to determine the upper and lower levels of the tool pin diameter according to Montgomery [14]. A pin diameter of 4 mm and a shoulder tool diameter of 14mm were used in this research. Other parameters such as the deviation angle equal to 3 degrees, and a 1.3 mm pin length and a shoulder tool entry in the joint instead of an axial force equal to 0.1 mm were used as a constant in all examinations. Finally, 36 examinations were experimentally executed with the mentioned constant parameters to determine the upper and lower levels of the linear speed travel of linear travel and the rotational speed of the tool.

In this research, a traditional milling machine was used as the friction stir welding machine. According to the milling machine facilities, applying an axial force to the tool during welding was not possible. A small entry of the shoulder tool in the joint can be considered as an alternative to the axial force. Depth of the shoulder tool entry was approximately 0.1 mm. Another important tool parameter was the cone. In this research, it was considered constant in all examinations (equal to 7 degrees).

In order to carry out an appropriate welding, it was necessary to join the plates firmly and to implement them in a proper fixed position by using a fixture. During the welding, the most important problem was the adhesion of the welding sheets to the bottom of the fixture. Talc powder was used to solve the problem; thus, before the welding procedure, the talc powder was uniformly sprayed between the bottom of the fixture and the welded sheets to prevent the adhesion of the sheets and the bottom of the fixture after welding. After the preparation of the friction stir welding instruments, the base metal was welded with different parameters such as the speed of rotation, speed of linear travel and different pin diameters. At the same time, using the DOE test design method through the Box-Behnken method [19], the optimum welding parameters were determined using the Montgomery method [14] and performing laboratory tests (Table. 1). These 17 tests were applied and the tensile strength for each test was obtained.

Table.1. Design of Experiments obtained by Box-Behnken method.

Number of Test	Rotation velocity (rpm)	Linear velocity (mm/min)	Pin diameter (mm)
1	750	160	5
2	500	95	5
3	750	95	4
4	1000	30	4
5	1000	95	3
6	500	160	4
7	1000	95	5
8	750	160	3
9	500	95	3
10	750	30	5
11	750	95	4
12	500	30	4
13	750	95	4
14	1000	160	4
15	750	30	3
16	750	95	4
17	750	95	4

Metallography tests were performed to study the microstructure of the base metal, weld metal, HAZ, TMAZ and also the microstructure developments. For this purpose, the samples were prepared and mounted with suitable dimensions. The target surfaces were polished by 80 to 3000 silicon carbide sandpapers and then polished by 0.3 micrometer alumina powder. The samples were etched for 30 seconds by using a 2% nital solution (2 ml solution of nitric acid in 98 ml of alcohol) where the low-carbon steel structure was bared and microstructures of the base metal and the weld zone were presented. The microstructure of different areas of the welded parts was investigated and analyzed at different magnifications by an Olympus optical microscope (model CK40M). For a better characterization of the microstructure and to obtain an elemental analysis, a scanning electron microscopy (SEM, model VEGA / TESCAN-XMU) equipped with chemical analysis (EDS) was used having a high resolution image (50000X) by point, line and map analysis. Mechanical tests including tensile test according to the ASTM-E8 standard were performed to investigate the mechanical properties using a tensile device (Model 4486 Instron). The micro hardness test using a micro hardness measurement device (Nexus Innova Test 4300) was performed on the welded specimens according to ASTM-E92 standard.

3. Results and Discussion

In this study, the optimum welding parameters were determined using the design of experiments method and laboratory tests. Applying different parameters to the workpiece, resulted in the joining of the parts with different heat inputs. An increase in the tool rotational speed as well as the tool shoulder diameter along with a decrease in the linear speed resulted in an increase in the friction which consequently resulted in the weld heat input. The pin diameter did not have much effect on the target function (not shown here). A lower linear speed travel and higher rotational speed resulted in higher weld strength. The reason could be seen in the friction and the heat generated in the welding. This strength has a maximum limit and increasing the friction more than the permissible limit, decreases the weld strength. Therefore, at first the optimum welding specimen was considered. The optimum welding parameters are presented in Table. 2.

Table. 2. The optimum welding parameters used.

Tensile Strength (MPa)	Pin Diameter(mm)	(mm/min)Linear Speed	Rotational Speed(rpm)
320	4	31.5	800

As can be seen in Fig. 1, in the welding sample using the optimum welding parameters, different zones with different properties at the jointing section are created due to the generated heat and mechanical operations. Fig. 2 shows the microstructure areas generated by the non-optimum parameters. It should be mentioned that the temperature in the SZ region was around 900-1000 °C. Therefore, the ferrite grains are expected to grow on the St37 side and get larger. On the other hand, by the rotation of the pin and shoulder in the SZ zone, the mechanical operation takes place which crushes and refines the grains up to 10-20 times and finally enhances the mechanical properties of the joint. TMAZ is located a little farther from the SZ, where it is simultaneously affected by the heat and mechanical operations however the amount was far less than that of the SZ. This resulted in structural refinement. Fig. 1 shows the TMAZ area. The HAZ area is located between the base metal and TMAZ. This zone becomes heat affected and no mechanical operation takes place in this area. In these areas, it was observed that in some parts, the grain size becomes more stretched and larger than the grain size of the base metal or at least the grain size of the HAZ which is equal to the grain size of the base metal. The reason could be that the increase of temperature and time could cause ferrite grain growth.

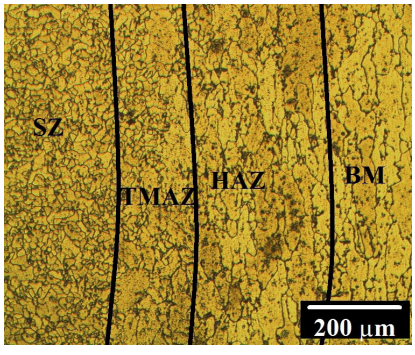

Fig. 1. Microstructure of the welded St37 steel in optimized state of the HAZ, TMAZ and SZ.

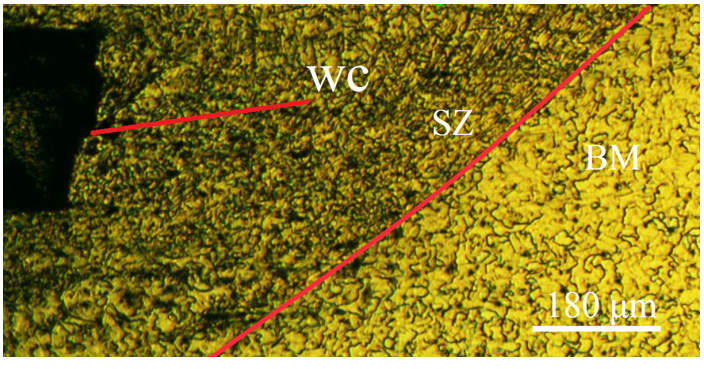

Fig. 2. Microstructure of the welded specimens using non-optimum parameters in the SZ and BM (The tungsten carbide is a contamination coming from the shoulder tool).

The friction stir welding parameters, especially the tool rotation speed and progressing speed could have a great impact on the mechanical and metallurgical properties of the joint. By investigating the microstructure of the base metal, it was observed that the microstructure of the St37 base metal was ferrite containing small amounts of pearlite. In order to measure the grain size, the Clemex software was used [20]. The grain size of ferrite is around 20 to 25 micrometers. However, the grain size in the TMAZ is reduced to around 5 to 10 micrometers due to the mechanical and thermal operations which cause the increase of strength according to the Hall-Petch equation and more flexibility due to the increase in grain boundaries [14]. This is clearly demonstrated in Fig. 3.

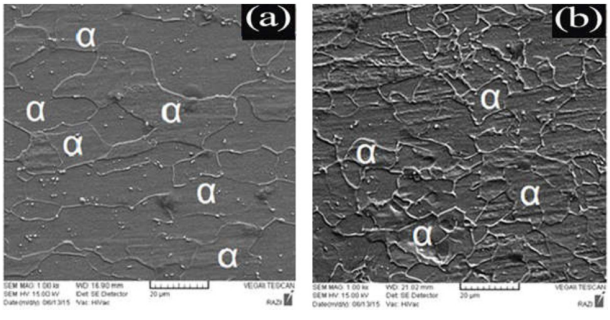

Fig. 3. SEM image of: a) St37 base metal and b) mechanical and heat-affected zone (in the figure, α ferrite zones have been shown).

Fig. 4(a) shows the SEM image of the 316L stainless steel microstructure. The matrix has an austenitic structure with coaxial grains. Since there are ferrite-forming elements such as Cr, Mo, and Si in the chemical composition of the 316L stainless steel, there is always some ferrite in the structure.

In Fig. 4(a), annealed twin structures could be seen. Such a structure is due to the dissolution annealing process after the rolling operation. Dissolution annealing is applied in order to dissolve the carbide precipitates that are formed during the hot rolling process. The TMAZ area mostly refers to the area located under the plastic deformation while dynamic re-crystallization has not occurred in the area.

Fig. 4 (b) shows the microstructure of the TMAZ region at the 316L stainless steel side. In this area, due to the thermal and mechanical operations the grains are refined and the strength has increased. Also, in Fig. 4(c), the interface of the welding and 316L base steel on the advancing side (AS) is observed and in Fig. 4(d), the interface of the weld metal and St37 stainless steel on the retreating side are shown.

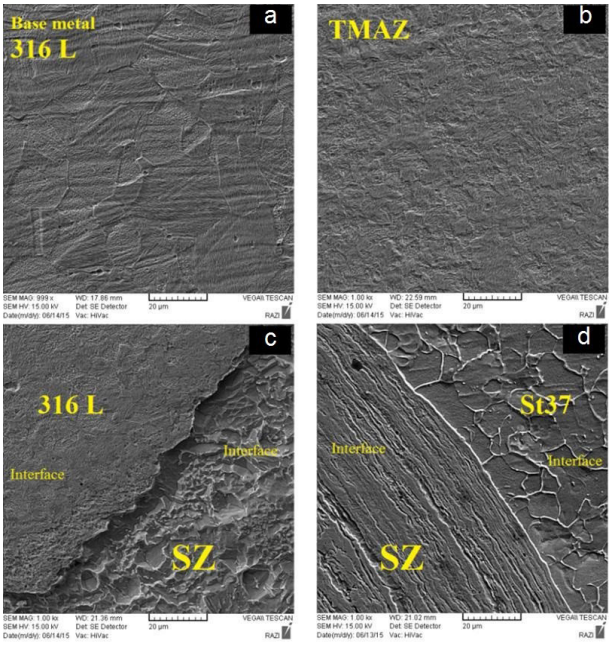

Fig. 4. The SEM image of the: a) 316L base metal, b) 316L mechanical and heat affected zones, c) the interface of 316L base metal and the SZ and d) the interface of St37 base metal and SZ.

Fig. 5(a) shows the SEM image with the optimum state parameters of St37 steel and the welding metal. The boundary between the St37 steel and welding metal is well defined. While Fig. 5(b) provides the elemental analysis, Fig. 6(a) shows a linear elemental analysis and Fig. 6(b) shows the microstructure of the interface. As expected, the distribution of the elements was roughly uniform while the increase in the iron element was observed by moving from the weld metal to the St37 steel. Also, there was no trace of the formation of chromium carbide in this area which could indicate the correct selection of the parameters for the friction stir welding process. Fig. 7(a) shows the elemental analysis results while Fig. 7(b) shows the SEM image of the interface of the 316L base metal and the weld metal. As can be seen, the greatest concentration gradient has occurred for iron and then chromium. Moving from the 316 L metal side to the weld metal and for the St37 metal, the iron content increased and the amount of chromium decreased.

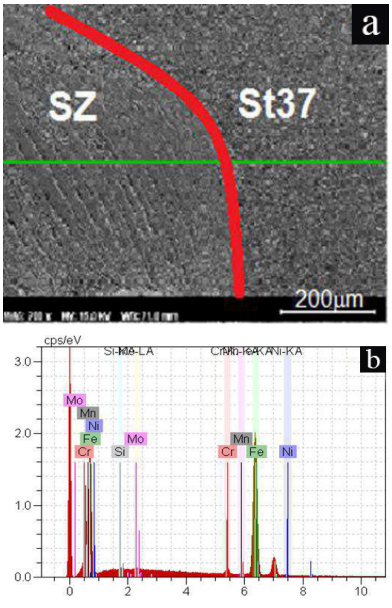

Fig. 5. The SEM image of: a) St37 base metal and weld metal interface and b) the elemental analysis results of the St37 base metal and weld metal interface.

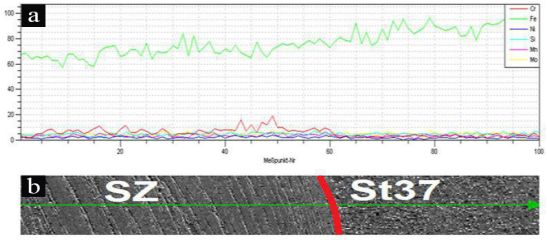

Fig. 6. The linear elemental analysis of the St37 base steel and weld metal interface.

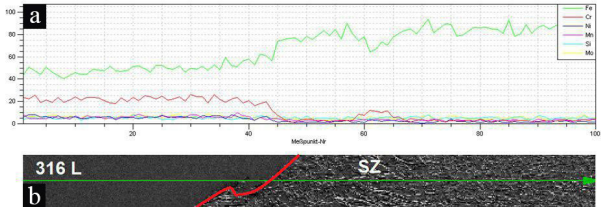

Fig. 7. a) Linear analysis of the 316L base metal and weld metal interface and b) the SEM microstructure of the 316L base metal and weld metal interface.

Figs. 8(a)-(d) show the image of the scanning electron microscope of the weld metal with different magnifications. According to Fig. 8, it appears that the weld zone in the joint has a layered structure and onion rings are formed in this weld. These alternating layers can be poor and rich-formed layers of alloying elements due to non-equilibrium cooling. Table. 3 shows the chemical composition of the elemental analysis of carbon, chromium, iron and nickel in accordance with Fig. 8(d). As can be seen, the percentages of carbon, nickel, and chromium are not very high. Since the structure is layered and alternate, the onion-shaped rings and alternating layers of poor and rich of alloying elements have been probably formed in the structure. Table. 4 shows the ultimate tensile strength results of the samples prepared using different processing parameters. By examining the fracture section of the samples in the tensile test, it was found that most of the welded specimens were broken from the retreating side of the base metal of the St37 steel side. The reason is that the St37 steel is weaker and therefore the rupture occurs on that part.

Table 3. The Spot analysis shown in the Fig. 8.

Spectra: CHROME CARBIDE

Element	Series	unn. C [wt.-%]	norm. C [wt.-%]	Atom. C [at.-%]
Carbon	K series	1.69	1.78	7.69
Chromium	K series	17.89	18.84	18.84
Iron	K series	66.58	70.11	65.26
Nickel	K series	8.81	9.27	8.21
	Total:	95.0 %		

Table. 4. Tensile test results of the welded sample using different parameters.

Sample code	Rotation Speed (rpm)	Linear travel speed (mm/min)	Ultimate tensile strength (MPa)	Sample failure location
a (316L)	---	---	520	Base metal
b (St37)	---	---	340	Base metal
c	800	31.5	320	Base metal
d	750	50	305	Base metal
e	800	50	310	Base metal
f	1000	31.5	280	Base metal
g	800	80	308	Base metal
h	500	31.5	200	Base metal

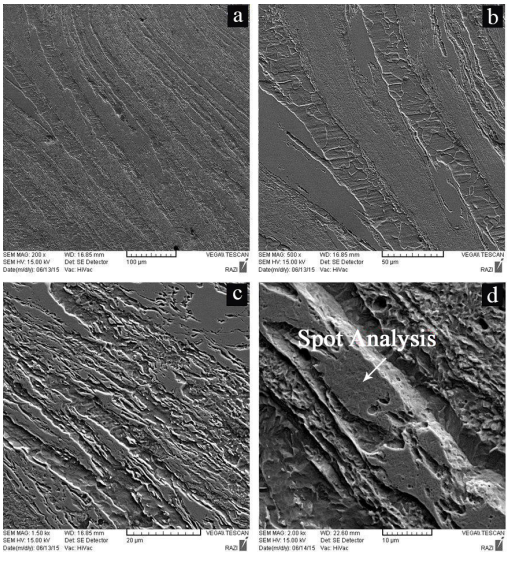

Fig. 8. The SEM image of the weld metal with different magnifications of: a)200X b)500X , c)1500X و d)2000X.

Fig. 9 shows the stress-strain diagram of the base metals and the welding sample using optimum parameters. As can be seen, the tensile strengths of the 316L base metal, the St37 base metal, and the welded sample are about 520, 340, and 320 MPa, respectively. This shows that the welding produced by the friction stir welding method, even under optimum parameters, has less strength compared with the base metals. However, the tensile strength with non-optimum parameters was even less than this value. Fig. 10 shows the micro-hardness results of the welded samples in accordance with the welding parameters of samples (e) and (c) according to Table 4. As can be seen in this Figure, the two welded steels are different in terms of hardness which is due to the non-uniformity and this difference is about 150HV. In sample (e) which has been welded with acceptable parameters, the hardness profile has relatively increased from St37 towards 316 L. As it is clear, due to the relative mixing of the two St37 and 316L steels, the hardness in the SZ region is much

lower than that of St37 and it is still less than 316 L. This is due to the microstructural changes that occurred during the welding process resulting in a sharp decrease in the grain size and, consequently, an increase in the hardness of the weld zone. Considering that sample (e) was welded at a rotation speed of 800 rpm and a linear travel of 50 mm/min, there is a lot of friction between the tool-metal work and the pin-metal work which results in increasing the pin temperature and the input heat in the work piece. In this case, since the pin rotates at a high speed in the stir area and then enters the welding zone, the tungsten particles enter the stir zone and form a composite of iron and tungsten and consequently, the localized hardness increases. Also, the thermo-mechanical operation has refined the grains. This raises the hardness in the stir zone and reduces the flexibility of the welding zone.

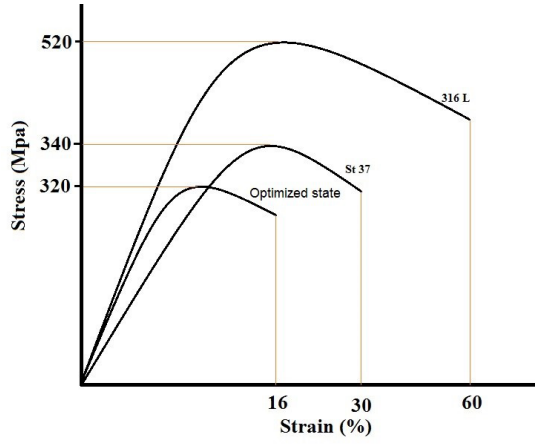

Fig. 9. The Stress-strain curves of the base metals and welded samples obtained using optimum parameters.

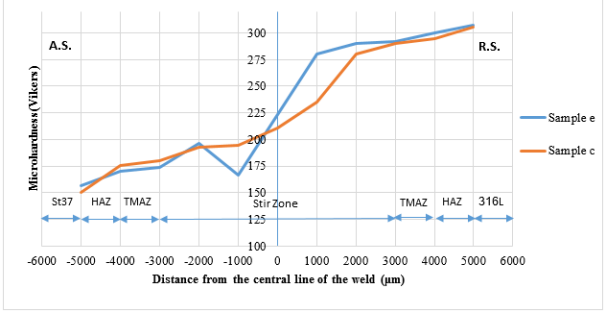

Fig. 10. Microstructure results of the welded samples in accordance with the welding parameters of samples (e) and (c) in Table. 4.

In sample (c), the parameters of the friction stir welding process have been tested according to the design software. In sample (c) for which the parameters of the friction stir welding process are determined by the design software and the optimum state was obtained, the minimum of the hardness range (150HV) was determined at the BM zone in the advancing side (AS) which matches the sample fracture location in the tensile test. In this sample, the input heat is optimized and the structure in the SZ zone is fine-grained due to thermo-mechanical operations therefore the hardness has increased in the area, and the value of hardness from the St37 steel side to the 316L steel side has approximately increased uniformly which could be a reason for the uniform distribution of the stir. In the TMAZ, because it is less affected by the thermo-mechanical process, compared to the SZ, it is more coarse-grained and the hardness increases with a slope less than the SZ. In the HAZ, due to the more coarsening of the grains, the hardness has increased unnoticeably.

4. Conclusion

Using the design of experiments method, the values of optimum friction stir welding parameters were obtained. The rotation speed and the linear travel speed are 800 rpm and 31.5 mm/min, respectively. The OM and SEM results of the welded samples with the optimum and non-optimum parameters all indicate that friction stir parameters have a significant impact on the quality and joint properties and that the choice of the value of these parameters is important. It was observed that in the SZ region, a mechanical operation was performed that caused the crushing and refining of the grains up to 10-20 times and consequently, the mechanical properties of the joint were enhanced. The TMAZ was less affected and caused the structure to refine. In the HAZ, no mechanical operation was performed and in some parts the grain size was elongated and became larger than the base metal grains. The SEM images of the welding showed that onion-shaped rings and alternative layers of poor and rich alloying elements were created which was due to the non-equilibrium cooling rate of the melt. The results of the tensile test indicated that the maximum tensile strength of 320 MPa was observed for the weld sample obtained using optimum parameters. The Vickers micro-hardness test in the sample with optimum parameters and acceptable parameters showed that the hardness of the samples increased from the St37 side to the 316L side and this increase in the sample with optimum parameters was more uniform.

References

[1] Y. Kiyohiro, N.Tsuda: Mater. Sci. Eng. A., 595(2014), 291.
[2] M. Burak, C. Meran: Mater. Design., 33(2012), 376.
[3] Y. Sato, M. Urata, H. Kokawa: Metall. Mater. Trans., 33(2002), 625.
[4] M. Jafarzadegan, AH. Feng, A. Abdolah-zadeh,

T. Saeid, J. Shen, H. Asadi: Mater. Characterization., 74(2012), 28.
[5] R. Kadaganchi, MR. Gankidi, H. Gokhale: Def. Techn., 11(2015), 210.
[6] R. Ueji, H. Fujii, L. Cui, A. Nishioka, K. Kunishige , K. Nogi: Mater. Sci. Eng., 423(2012), 324.
[7] T. Hirata, T. Oguri, H. Hagino, T. Tanaka, SW. Chung, Y. Takigawa, K. Higashi: Sci. Eng. A., 456 (1-2) (2007), 344.
[8] Montgomery DC Design and Analysis of Experiments, Vol ISBN. 0-471-48735-X. Sixth Edition edn. John Wiley & Sons. Inc (2005).
[9] YS. Sato, H. Kokawa: Metallurgical and Materials Transactions A30 (12) (1999),3125.
[10] G. Elatharasan,VSS. Kumar: Procedia Eng., 38(2012), 3479.
[11] C Elanchezhian, B. V. Ramnath, P. Venkatesan, S. Sathish, T. Vignesh, RV. Siddharth, B. Vinay, K. Gopinath: Procedia Eng., 97(2014), 778.
[12] G. Rambabu, D. B. Naik: Rao CHV, K.S. Rao, G. M. Reddy: Def. Techn., 11(2015), 335.
[13] C. Meran, V. Kovan, A. Alptekin: Friction stir welding of AISI 304 austenitic stainless steel. Mat-wiss u Werkstofftech, 38(2007).
[14] Design Expert Software. 7.1.6 edn. Stat Ease Inc, Minneapolis, MN.
[15] Y. Sankara, J. Venumurali, G. Sivaramudu, K. Saraswathi :(2017) A Study to Optimize Process Parameters of FSW Joints by Using Design-Expert and Fuzzy-Approach. 6:17930.
[16] SLC. Ferreira, RE. Bruns, HS. Ferreira, GD. Matos, JM. David, GC. Brandao, EGPd. Silva, LA. Portugal, PSd. Reis, AS. Souza, WNLd. Santos:. Analytica Chimica Acta., 597(2007), 179.
[17] CLEMEX software. version 4.0 edn. Captiva v4.0 software (Clemex Technologies, Inc.).